BIOLOGY OF REPRODUCTION (2013) **88**(6):141, 1–9
Published online before print 17 April 2013.
DOI 10.1095/biolreprod.112.107110

t-SNARE Syntaxin2 (STX2) Is Implicated in Intracellular Transport of Sulfoglycolipids During Meiotic Prophase in Mouse Spermatogenesis[1]

Yasuhiro Fujiwara,[3,5] Narumi Ogonuki,[4] Kimiko Inoue,[4] Atsuo Ogura,[4] Mary Ann Handel,[5] Junko Noguchi,[6] and Tetsuo Kunieda[2,7]

[3]*Graduate School of Natural Science and Technology, Okayama University, Okayama, Okayama, Japan*
[4]*RIKEN BioResource Center, Tsukuba, Ibaraki, Japan*
[5]*The Jackson Laboratory, Bar Harbor, Maine*
[6]*Animal Development and Differentiation Research Unit, National Institute of Agrobiological Sciences, Tsukuba, Ibaraki, Japan*
[7]*Graduate School of Environmental and Life Science, Okayama University, Okayama, Okayama, Japan*

ABSTRACT

Syntaxin2 (STX2), also known as epimorphin, is a member of the SNARE family of proteins, with expression in various types of cells. We previously identified an ENU-induced mutation, *repro34*, in the mouse *Stx2* gene. The *Stx2*^{repro34} mutation causes male-restricted infertility due to syncytial multinucleation of spermatogenic cells during meiotic prophase. A similar phenotype is also observed in mice with targeted inactivation of *Stx2*, as well as in mice lacking enzymes involved in sulfoglycolipid synthesis. Herein we analyzed expression and subcellular localization of STX2 and sulfoglycolipids in spermatogenesis. The STX2 protein localizes to the cytoplasm of germ cells at the late pachytene stage. It is found in a distinct subcellular pattern, presumably in the Golgi apparatus of pachytene/diplotene spermatocytes. Sulfoglycolipids are produced in the Golgi apparatus and transported to the plasma membrane. In *Stx2*^{repro34} mutants, sulfoglycolipids are aberrantly localized in both pachytene/diplotene spermatocytes and in multinucleated germ cells. These results suggest that STX2 plays roles in transport and/or subcellular distribution of sulfoglycolipids. STX2 function in the Golgi apparatus and sulfoglycolipids may be essential for maintenance of the constriction between neighboring developing spermatocytes, which ensures ultimate individualization of germ cells in later stages of spermatogenesis.

glycolipids, meiosis, mouse, spermatogenesis, Stx2

INTRODUCTION

Spermatogenesis consists of a series of mitotic and meiotic cell divisions that maintain germ cells connected by narrow intercellular bridges. After differentiation of haploid spermatids, the individual germ cells are released from the seminiferous epithelium. The full spectrum of genes that regulate these processes of proliferation and differentiation is not fully known. To identify previously unknown mouse genes responsible for spermatogenesis, an unbiased strategy of ENU mutagenesis was employed, followed by screening for phenotypes of arrested spermatogenesis and infertility [1]. Several novel genes involved in fertility were discovered [2, 3]. Among the mutations causing male-restricted infertility, we previously positionally localized the *repro34* mutation in the mouse genome, identifying the *Stx2* gene, encoding syntaxin 2 (STX2), also known as epimorphin [4]. The *Stx2*^{repro34} mutants exhibit arrest of spermatogenesis at meiotic prophase, and the multinucleation of mutant germ cells suggests roles for this protein in membrane functions and/or intercellular bridges.

STX2 is one of the SNARE (soluble *N*-ethylmaleimide-sensitive factor attachment protein receptor) family members. Many SNARE family proteins are involved in membrane trafficking pathways during cytokinesis in a variety of organisms [5]. In somatic cytokinesis, STX2 is essential for abscission of the midbody, the connecting bridge of two daughter cells [6]. Expression of STX2 is also evident in reproductive cells, including acrosomes of spermatozoa, where it induces the membrane fusion required for the acrosome reaction and release of acrosomal components during fertilization [7, 8].

Mice deficient in STX2, both the targeted *Stx2* knockout mice [9] and *Stx2*^{repro34} homozygotes [4], exhibit spermatogenesis arrested at meiotic prophase, with the formation of multinucleated spermatocytes. Therefore, in addition to its acrosomal function, STX2 appears to be crucial for membrane dynamics that maintain intercellular germ cell bridges during spermatogenesis. Interestingly, mice deficient in sulfoglycolipids exhibit a similar germ cell multinucleation phenotype [10, 11]. The testis is rich in sulfoglycolipids, and 90% of the sulfated glycolipids are from seminolipid, a glycolipid predominantly found in testis [12]. Sulfoglycolipid biosynthesis is regulated by both ceramide galactosyltransferase (CGT, also known as UDP galactosyltransferase 8A, UGT8A) and cerebroside sulfotransferase (CST, also known as glastose-3-O-sulfotransferase 1, GAL3ST1). Seminolipid is a component of the lipid rafts in the sperm head membrane that function in sperm attachment to the zona pellucida during fertilization [13]. Genetic deficiency of either CGT [10] or CST [14] results in complete deficiency of sulfoglycolipids in the testis, and spermatogenesis is impaired in these mutants. Transplantation assays revealed that the spermatogenesis defects in CST-deficient mice are intrinsic to germ cells, as seminolipid-deficient somatic components could support spermatogenesis [11]. Multinucleation of germ cells is a distinct feature common to both CST and CGT seminolipid-deficient models [10, 11, 14]. Multinucleation of the germ cells is also often

[1]Supported by Japan Society for the Promotion of Science (JSPS), Strategic Young Researcher Oversea Visits Program for Acceleration Brain Circulation.
[2]Correspondence: Tetsuo Kunieda, Okayama University, 1-1-1 Tsushima-naka, Kita-ku, Okayama 700-8530 Japan.
E-mail: tkunieda@cc.okayama-u.ac.jp

Received: 18 December 2012.
First decision: 15 January 2013.
Accepted: 9 April 2013.

eISSN: 1529-7268 http://www.biolreprod.org
ISSN: 0006-3363

found in pathological testicular conditions, presumably due to the opening of intercellular bridges. These germ cell bridges are stable cytoplasmic extensions and interconnect large numbers of spermatogenic cells during their synchronous differentiation [15]. Multinucleation of somatic cells is caused by two mechanisms: cell-cell fusion and acytokinetic cell division [16]. Although intercellular bridges in germ cells have distinct functions different from the interconnections in somatic cells, the molecular mechanisms that form the intercellular bridges are shared [17]. Moreover, recent studies have suggested that lipid raft domains within membranes play an important role in regulation of cytokinesis [18].

In this study, we used *Stx2*^{repro34} mutant male mice to determine a common cellular phenotype underlying the multinucleation of germ cells in STX2 and seminolipid deficiencies, especially in breakage or loss of stability of the intercellular bridges. We show that the target-SNARE (t-SNARE) STX2 is required for maintenance of germ cell intercellular bridges during the meiotic prophase of spermatogenesis, and that it contributes to intracellular and membrane localization of sulfoglycolipids.

MATERIALS AND METHODS

Animals

The *Stx2*^{repro34} mice used were originally produced by the National Institutes of Health-supported Reproductive Genomics program at the Jackson Laboratory. The *repro34* mutation was induced in a C57BL/6J background and subsequently outcrossed to C3HeB/FeJ; a *Stx2*^{repro34}-C3HeB/FeJ congenic line was created. For experimental analyses, *Stx2*^{repro34} homozygotes and control wild-type littermates were selected at 10–12 wk of age, or at 1–5 wk of age to follow the first wave of spermatogenesis. The genotyping protocol for *Stx2*^{repro34} was described previously [4]. Rats from a Jcl:Wister closed colony at 9–10 wk of age were purchased from CLEA Japan. All the experiments using animals were approved by the animal care and use regulatory committees of both Okayama University and The Jackson Laboratory.

Cytological Preparations and Immunostaining

Histology. Testes from mice and rats were fixed in Bouin solution or 4% PFA fixative (4% paraformaldehyde, 0.1 M phosphate buffer, pH 7.4) and paraffin embedded. Sections (5 μm) were stained with hematoxylin and eosin for evaluation of spermatogenesis. For immunostaining, sections were autoclaved in 0.1 M sodium citrate (pH6.0) at 120°C for 20 min or treated with 20 μg/ml proteinase K in 10 mM Tris-HCl (pH 7.4) at 37°C for 20 min for antigen retrieval, if necessary. All sections were incubated in 3% H_2O_2 in PBS for 15 min to quench the endogenous peroxidase, and subsequently incubated in PBS containing 10% bovine serum albumin (BSA) for 30 min at room temperature (RT). Primary antibodies (Supplemental Table S1; all Supplemental Data are available online at www.biolreprod.org) diluted with PBS containing 1% BSA were applied, and slides were incubated for 3 h at 37°C. The horseradish peroxidase (HRP)-labeled secondary antibodies (Santa Cruz) were applied at 1:400 dilution for 1 h at RT. Antigens were visualized using the TSA Plus DNP (HRP) System (Perkin Elmer) with NEL 747B Dako Liquid DAB+ Substrate Chromogen System (20 μl/ml; K3467; DAKO). Sections were counterstained with hematoxylin. Immunostaining of sulfoglycolipids was undertaken following the method previously described [19]. Briefly, testes were fixed in 4% PFA, and the fixative was replaced with an increasing gradient (12%–18%) of sucrose in Hanks balanced salt solution (137 mM NaCl, 5 mM KCl, 0.44 mM KH_2PO_4, 5.6 mM glucose, 0.34 mM Na_2HPO_4 anhydrous, 0.81 mM $MgSO_4$, 1.26 mM $CaCl_2$, and 4.17 mM $NaHCO_3$). Tissue samples were embedded in OCT compound and frozen. Frozen tissues (7 μm) were incubated with a monoclonal mouse DI8 antibody in PBS containing 5% skim milk for 3 h at 37°C. The secondary antibody, goat anti-mouse IgG-Alexa Flour 488 (1:200 dilution; A-21121; Invitrogen), was applied with the same buffer as the primary antibody and incubated for 1 h at RT. The nuclei were counterstained with DAPI (4′,6-diamidino-2-phenylindole), mounted using VECTASHIELD Mounting Medium (H-1200; Vector Laboratories Inc.), and observed using a BIOREVO BZ-9000 (Keyence) microscope system. Colocalization of STX2 and TEX14 was examined in paraffin sections of testes fixed in Bouin solution. Following incubation with the primary antibodies, sections were incubated with secondary antibodies donkey anti-goat IgG-DyLight 488 (1:500 dilution; 705-485-003; Jackson ImmunoResearch) and donkey anti-rabbit IgG-Cy3 (1:500 dilution; 711-165-152; Jackson ImmunoResearch). The nuclei were counterstained with DAPI, mounted using VECTASHIELD Mounting Medium, and observed as described above.

Squash preparations. Squash preparations of germ cells were prepared based on the previously described method, with some modifications [20]. Briefly, mouse testes were placed in PBS and decapsulated. Seminiferous tubules were cut into segments 1–2 mm in length, and both ends were removed for identification of the stages of spermatogenesis. The middle of each tubular segment was used for immunocytochemistry. The segments (0.5 mm) were placed in 15 μl of 100 mM sucrose on a glass slide, and squashing with a coverslip caused the cells to flow from the tubule. The slide was quickly dipped in liquid nitrogen for 20 sec, and the coverslip was removed using a scalpel. The slides were then fixed with 4% PFA in PBS for 15 min at RT, followed by treating with 0.1% Triton X-100 in PBS for 10 min at RT. After washing twice in PBS and blocking with 5% skim milk in PBS, the slides were incubated with primary antibodies in 5% skim milk in PBS to examine colocalization of STX2 with TEX14, or of sulfoglycolipids with TEX14. The secondary antibodies were donkey anti-rabbit IgG-Cy3 (1:500 dilution; 711-165-152; Jackson ImmunoResearch) and donkey anti-goat IgG-DyLight488 (1:500 dilution; 711-485-033; Jackson Immuno Research), and goat anti-mouse IgG-Alexa Flour 488 (1:500 dilution; A-11001; Invitrogen) and donkey anti-goat IgG-Alexa Flour 568 (1:500 dilution; A-11057; Invitrogen), respectively. The nuclei were counterstained with DAPI, then mounted using VECTASHIELD Mounting Medium and observed as described above.

Surface spread preparations. Surface spread preparation of testicular cells was prepared as previously described, with some modifications [21–23]. Briefly, cells were collected in Dulbecco modified Eagle medium (12100-046; Invitrogen). After centrifugation at 1800 rpm for 10 min at 4°C, pelleted cells were suspended in 0.5% NaCl solution and spread on a glass slide. The preparation slides were soaked in 2% PFA containing 0.02% SDS in PBS (pH was adjusted to 7–8 with 0.1 M $Na_2B_4O_7$). After washing with PBS containing 0.04% DRIWEL (Fuji photo film co., LTD), the preparation slides were blocked with antibody dilution buffer (ADB; PBS containing 2% BSA and 0.05% Triton-X 100) and then incubated with polyclonal guinea pig anti-SYCP3 and monoclonal mouse anti-γH2AX in PBS containing 10% ADB overnight at 4°C. Slides were then incubated with secondary antibodies goat anti-mouse IgG-Alexa Flour 488 (1:200 dilution; A-21121; Invitrogen) and goat anti-guinea pig IgG-Alexa Fluor 594 (1:200 dilution; A11076; Invitrogen) in PBS containing 10% ADB for 1 h at RT. The slides were mounted with VECTASHIELD Mounting Medium and observed.

Chromosome preparations. The procedure for chromosome preparations and identification of cell stages was as previously described [24–27], with some modifications. Briefly, the seminiferous tubules of the testes were placed in 20 ml of 2.2% sodium citrate. A cluster of seminiferous tubules was disentangled and treated with 1% sodium citrate hypotonic solution for 30 min at RT, and subsequently replaced with fixative (methanol-acetic acid ratio = 3:1) for 10 min at 4°C. The fixed tubules were transferred to 50% acetic acid until germ cells were dispersed. Cells were collected by centrifugal separation at 1500 rpm for 10 min and resuspended in the same fixative as previously. A few drops of cell suspension were dropped on a glass slide and air-dried. The slides were stained with 5% Giemsa-solution for 5 min.

Preparations of structurally preserved cells were made as previously described [28], with some modifications. Testes were dissected and placed into test tubes containing 1 ml of ice-cold Ringer solution (155 mM NaCl, 5.6 mM KCl, 2.2 mM $CaCl_2$, and 2.4 mM $NaHCO_3$) for 4 h, and minced in the microtubule-stabilizing buffer (100 mM PIPES [piperazine-N,N′-bis(2-ethanesulfonic acid); pH 6.8], 1 mM $MgSO_4$, 1 mM ethylene glycol tetraacetic acid, and 1% Triton X-100). After centrifuging at 1500 rpm for 5 min, the resulting germ cell suspension was spread onto slides. The slide preparations were placed in fixative (0.25% glutaraldehyde and 2% formaldehyde, in the microtubule-stabilizing buffer without detergent) for 30 min. For further stabilization of cytoskeletons, slides were immersed in methanol at −20°C. The preparation was then treated with $NaBH_4$ (0.5 mg/ml in PBS), washed with PBS containing 0.02% NaN_3 and 0.1% Triton X-100, and then with the same solution without the detergent. The cells were incubated with polyclonal rabbit anti-α-TUBULIN antibody, and subsequently with goat anti-mouse IgG-Alexa Flour 488 secondary antibody (1:500 dilution; A-11001; Invitrogen). The slides were sealed with VECTASHIELD Mounting Medium with DAPI and observed as above.

Western Blot Analysis

Testes removed from *Stx2*^{repro34} homozygous and normal mice were homogenized in radioimmunoprecipitation assay buffer (150 mM NaCl, 10 mM Tris-HCl [pH 7.2], 0.1% SDS, 1.0% Triton X-100, 1% deoxycholate, and 5 mM EDTA). The protein concentration of cell lysate was measured using the

bicinchoninic acid protein assay kit (B9643; Sigma), and 50 μg of total protein was applied on 10% SDS-polyacrylamide gels for electrophoresis and transferred onto Immobilon-P Transfer Membranes (Millipore). The membrane was incubated with polyclonal goat anti-epimorphin antibody (1:500 dulution; BAF2568; R&D Systems) and polyclonal rabbit anti-βactin antibody (1:1000 dilution; ab8227; Abcam), and subsequently with HRP-conjugated anti-goat or anti-rabbit IgG secondary antibodies (1:20 000 dilution; Santa Cruz). The membrane was developed using ECL Advance Western Blotting Detection Kit (RPN2135; Amersham Biosciences) and observed.

Round Spermatid Nuclear Injections and Chromosome Analyses

Round spermatid injection. Round spermatid injection (ROSI) using nuclei of the mutant syncytial germ cells was undertaken following the method previously described [29], with some modifications. Testes were placed in erythrocyte-lysing buffer (155 mM NH_4Cl, 10 mM $KHCO_3$, and 2 mM ethylenediaminetetraacetic acid; pH7.2). The seminiferous tubule masses were transferred into cold GL-PBS (PBS containing 5.6 mM glucose, 5.4 mM sodium lactate, and 0.1 mg/ml of polyvinylpyrrolidone). The cell suspension in GL-PBS was filtered and collected by centrifugation at 800 rpm for 4 min. Recipient eggs were prepared from 9- to 12-wk-old BDF1 mice that were injected with 7.5 IU of equine chorionic gonadotropin, and an additional 7.5 IU of human chorionic gonadotropin (hCG) 48 h later. Mature oocytes were collected from the oviducts 15–17 h after hCG injection and were freed from cumulus cells by treatment with 0.1% hyaluronidase in CZB medium [30]. The oocytes were then transferred to fresh CZB and incubated at 37°C in 5% CO_2 condition for 90 min before ROSI.

ROSI was performed following the standard method for a Piezo-driven micromanipulator (Prime Tech Ltd.) [29]. Syncytial cells that were smooth ovoid-shaped as well as relatively rich in the cytoplasm and with clear nucleoli in the nuclei (see Supplemental Fig. S5B) were regarded as healthy; the nuclei from these were used as donors. In 40–60 min after activation of oocytes with Ca-free CZB containing 2.5 mM $SrCl_2$ for 20 min at 37°C, the oocytes at telophase II were microinjected with the nucleus of the mutant syncytial germ cell. After injection, oocytes were kept in Hepes-CZB for 10 min at RT and then cultured in CZB at 37°C. Embryos that reached the 2-cell or 4-cell stages after 48 h of culture were transferred into the oviducts of the pseudopregnant Jcl:ICR female mice (8–12 wk old). On Day 19.5 after transplantation, the recipient mice were examined for live term fetuses or traces of implantation.

Chromosome preparations from microinjected embryos. For chromosome analysis of *Stx2*^{repro34} mutant male donor nuclei, the eggs were transferred into CZB 3–4 h after the microinjection and cultured for 17–20 h. Subsequently, they were treated in CZB containing 0.5% pronase for 5–10 min and washed with CZB medium for 10 min prior to hypotonic treatment. After washing with hypotonic solution (1:1 = 1% sodium citrate in distilled water, 30% fetal calf serum in distilled water) in the first well of three-bored hollow glass, the ova were transferred into the second and third wells containing the same hypotonic solution and incubated for 10 min in each. The hypotonic solution-treated ova were transferred to the third well containing 1 ml of the first fixative (methanol-acetic acid-water ratio = 5:1:4) and incubated for 5–10 min. The ova were then transferred to a clean slide and fixed with the second fixative (methanol-acetic acid ratio = 3:1) and then the third fixative (methanol-acetic acid-water ratio = 3:3:1) sequentially. The fixative was evaporated on the water bath set at 60°C for 20 min and dried. The preparation slides were stained with filtered 4% Giemsa solution and observed using an Eclipse E800 microscope (Nikon).

RESULTS

Abnormal First Wave of Spermatogenesis in Stx2^{repro34} *Mutants*

Analysis of prepubertal testes revealed that syncytial multinucleated germ cells appear in the *Stx2*^{repro34} mutants during the first wave of spermatogenesis. At Day 16 postbirth (P16), spermatocytes advanced up to mid- and late pachytene stages (Fig. 1D). Neither round nor elongated spermatids were observed in the mutant at P32 (Fig. 1F), while mature spermatozoa were produced in wild type (Fig. 1F). Although the *Stx2*^{repro34} mutant males were indistinguishable from the wild-type males in growth, testicular weights of the mutants were significantly lower at times later than P16 (Supplemental Fig. S1).

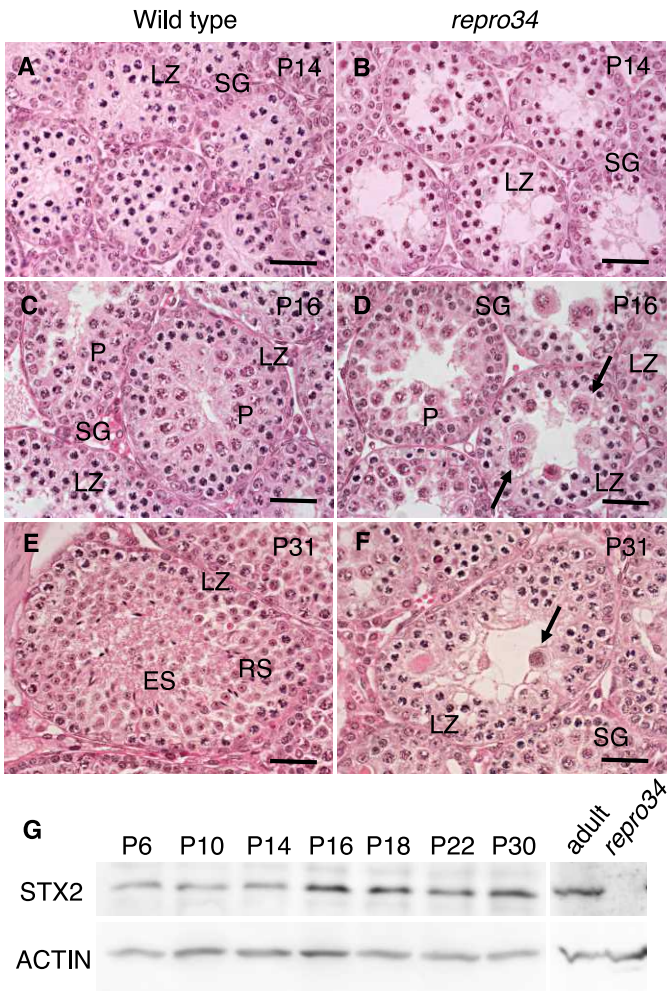

FIG. 1. First wave of spermatogenesis of the *Stx2*^{repro34} mutant and STX2 expression. **A**, **B**) At P14, no significant differences were observed between wild-type (**A**) and *Stx2*^{repro34} mutants (**B**). **C**, **D**) At P16, pachytene spermatocytes were observed in normal testes (**C**), and the mutant testes included syncytial multinucleated spermatocytes (**D**, arrows). **E**, **F**) At P32, the seminiferous epithelium in wild type was filled with round and elongating spermatids (**E**), whereas no spermatids were observed in the seminiferous epithelium of the mutants (**F**). Arrows in **F** indicate multinucleated cells. **G**) Western blotting of STX2 in the testis revealed a weak expression at P6–P14. At P16 and later days, higher expressions were seen. No expression was detected in the adult mutant testis. SG, spermatogonia; L/Z, leptotene or zygotene spermatocytes; P, pachytene spermatocyte; RS, round spermatid; ES, elongated spermatid. Arrows indicate degenerated germ cells. Bar = 100 μm.

Expression of STX2 protein was detected throughout the first wave of spermatogenesis in wild-type testes, with a marked increase at P16, when pachytene spermatocytes are abundant, and was sustained thereafter (Fig. 1G). No STX2 protein was detected in *Stx2*^{repro34} mutant testes (Fig. 1G).

Multinucleated Germ Cells in Stx2^{repro34} *Mutants*

In assessing the morphology of the multinucleated germ cells in the *Stx2*^{repro34} mutant, immunohistochemistry of LAMIN-B1 revealed integrity of the nuclear membrane (Supplemental Fig. S2B inset). Normal stage-specific expression of γH2AX was observed in the nuclei of both wild-type pachytene spermatocytes (Supplemental Fig. S2C) and the syncytial mutant pachytene spermatocytes (Supplemental Fig. S2D), in accordance with previous staging [31]. The intercellular bridges are

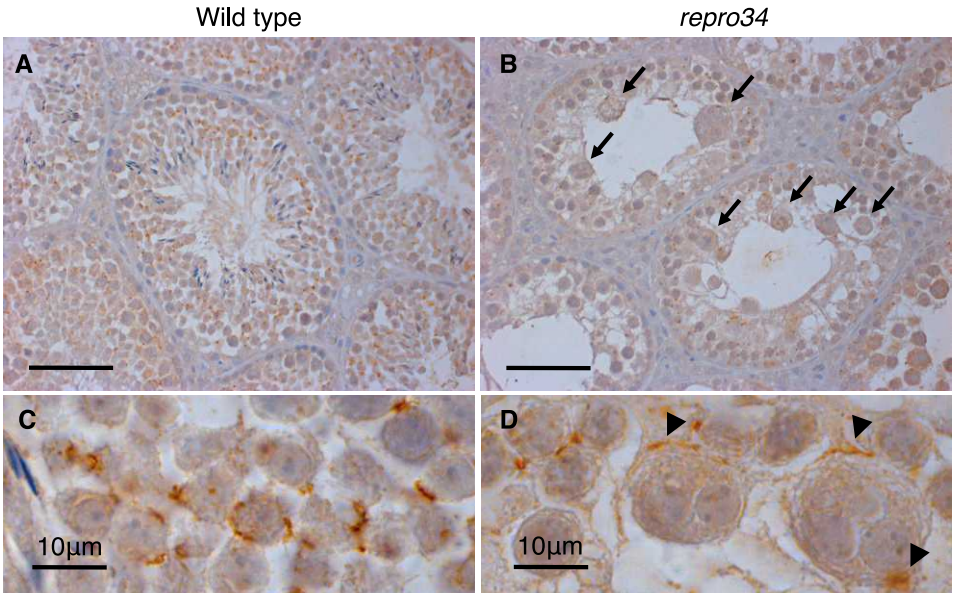

FIG. 2. Immunohistochemical analysis of *Stx2*^{repro34} mutant testis. **A**–**D**) The ring-shaped expression of TEX14, a component of the intercellular bridge of germ cells, was observed in the connecting regions of the cells in both wild-type (**A**, **C**) and mutant testis (**B**). Note positive reactions around multinucleated germ cells (**D**, arrowheads). Arrows in **B** indicate multinucleated cells. Bars in **A** and **B** = 50 μm.

open channels between clonal spermatogenic cells [32, 33], and TEX14 is one of the bridge-specific proteins [34]. Localization of TEX14 around the spermatogonia, spermatocytes, and spermatids confirmed the presence of the bridges between the germ cells in the wild type (Fig. 2, A and C). This was also observed in mutant testes, in cells with no morphological abnormalities (Fig. 2, B and D). However, mutant multinucleated cells, in which bridges were not maintained, displayed aberrant localization of TEX14 in a patchy pattern (Fig. 2D). This data reveal abnormalities of *Stx2*^{repro34} spermatocytes before meiotic metaphase.

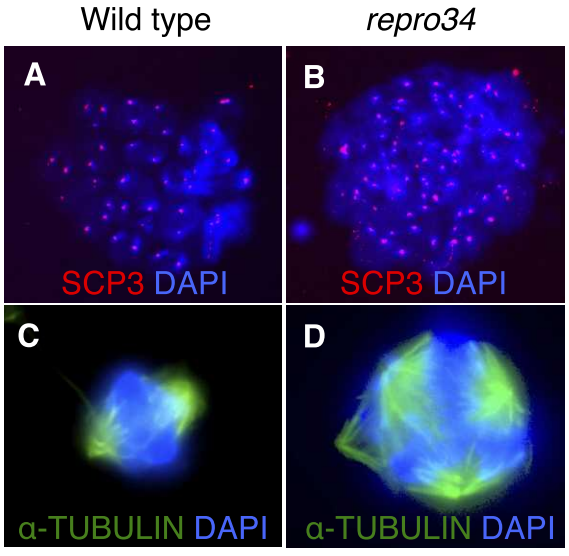

FIG. 3. Multinucleation and chromosomes. Germ cells collected by squash technique from the wild-type (**A**, **C**) and *Stx2*^{repro34} mutant testes (**B**, **D**) were immunostained with antibodies against SCP3 (**A**, **B**) and α-TUBULIN (**C**, **D**). **A**, **B**) Spots of SCP3 in metaphase spermatocyte showed chiasma formation (red spots in **A** and **B**). Note more spots were observed in the mutant than in the wild type (**B**). **C**, **D**) Spindle formation in metaphase spermatocyte was shown by α-TUBULIN. Wild-type metaphase spermatocyte showed a single pair of spindle bodies (**C**), while multipolar formation of spindle bodies was observed in the mutant syncytial cell (**D**). The nuclei were counterstained with DAPI. Original magnification ×1000.

Metaphase spermatocytes in wild-type testes had localization of SYCP3 to centromeres and the normal number of chromosome (2n = 40; Fig. 3A), as described previously [35]. However, consistent with multinucleation, spermatocytes in *Stx2*^{repro34} mutant testes displayed SYCP3 localization in double or triple the normal number of spots (Fig. 3B). Multinucleated metaphase spermatocytes also exhibited a multipolar formation of the spindles (Fig. 3D) and multiploidy of the metaphase spermatocytes (Supplemental Fig. S3). A TUNEL assay showed a frequent apoptosis of the multinucleated metaphase spermatocytes (data not shown).

We tested developmental competence of the nuclei in the syncytial cells using ROSI (Supplemental Fig. S4, B and C). With injection of nuclei from wild-type round spermatids, 31.0% of transplanted embryos developed normally. However, when nuclei from mutant multinucleated mutant cells were injected, no embryos developed normally and no offspring were obtained (Supplemental Table S2). We analyzed chromosome preparations from eggs injected with nuclei from the *Stx2*^{repro34} multinucleated germ cells. Among 32 male pronuclei, 23 contained chromosomes, most likely from primary spermatocytes, with metaphase I-like bivalents apparent (Supplement Fig. S4D). Another six nuclei contained chromosomes appearing to be from somatic cells, and three pronuclei were uncountable. We found no male pronuclei with a normal haploid set of chromosomes. These data are consistent with arrest of *Stx2*^{repro34} spermatocytes before the MII division and aquisition of developmental completence.

Expression and Subcellular Localization of t-SNARE STX2 in the Golgi Apparatus and Intercellular Bridges

Since STX2 is an element in the midbody and cytoplasmic bridges of somatic cells [6], we assessed whether the protein localizes to the intercellular bridges of spermatogenic cells. In testicular cross sections, STX2 was observed in intercellular

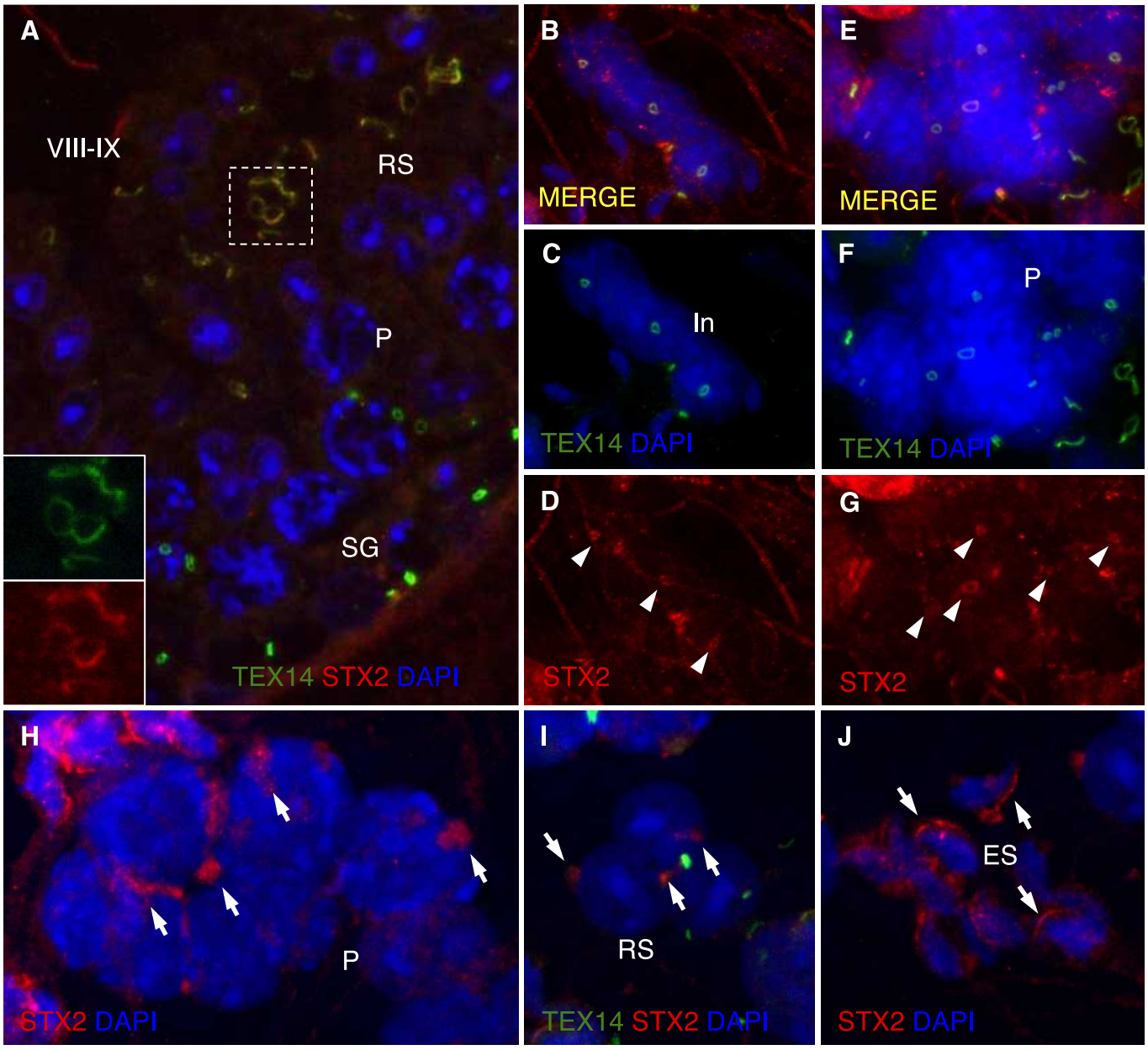

FIG. 4. Subcellular localization of STX2 in the developing germ cells. **A**) In the testicular section, STX2 (red) and TEX14 (green) were colocalized to the intercellular bridges of the spermatids (**A**, inset). **B–G**) Germ cells obtained from the seminiferous tubular segment at stages I–IV by squash preparation revealed localization of STX2 to the intercellular bridges of spermatogonia and pachytene spermatocytes (arrows in **D** and **G**, respectively), which was colocalized with TEX14 (**B**, **E**). **H–J**) Subcellular localization of STX2 was observed in the perinuclear region of pachytene spermatocytes obtained from the segment at stages IX–X (**H**). The proacrosomal region of round spermatids from the segment at stages I–VII (**I**) and the acrosomes of elongated spermatids from post-stage VIII (**J**) also exhibited STX2 localization. Arrows in **H** indicate perinuclear localization of STX2, arrows in **I** indicate localization of STX2 to the proacrosomal region, and arrows in **J** indicate acrosomal localization of STX2. Nuclei were counterstained with DAPI. Roman numerals show stages of the spermatogenic cycle. SG, spermatogonia; In, intermediate spermatogonia; P, pachytene spermatocytes; RS, round spermatid; ES, elongated spermatid. Original magnification ×400 (**A**) and ×1000 (**B–J**).

bridges both between spermatocytes and between spermatids (Fig. 4A; Supplemental Fig. S5C, inset). STX2 was colocalized with TEX14, a known protein marker of bridges between spermatogenic cells (Fig. 4A). Intercellular bridges are known to increase in diameter as germ cells differentiate, being approximately 1–1.3 μm in spermatogonia, 1.4–1.7 μm in spermatocytes, and ≥1.8 μm in spermatids [33]. We observed a similar pattern of increase of diameter in the STX2 localization pattern. We did not observe any consistent or definitively positive reaction for STX2 in the testicular interstitial tissue. To optimize visualization of STX2 in bridges between spermatogonia, we utilized squash preparations of germ cells. In immunostained germ cells from stage II–IV seminiferous tubule segments, STX2 was localized to bridges between intermediate spermatogonia (Fig. 4, B–D) and between early pachytene-stage spermatocytes (Fig. 4, E–G). However, signal intensity for STX2 was not as strong in these cells as it was in late pachytene spermatocytes and spermatids. Examination of germ cells released from stage IX–X tubule segments revealed that STX2 was localized to the perinuclear region (Fig. 4H), and also to the proacrosome and acrosome regions in round and elongating spermatids, respectively (Fig. 4, I and J). Addition-

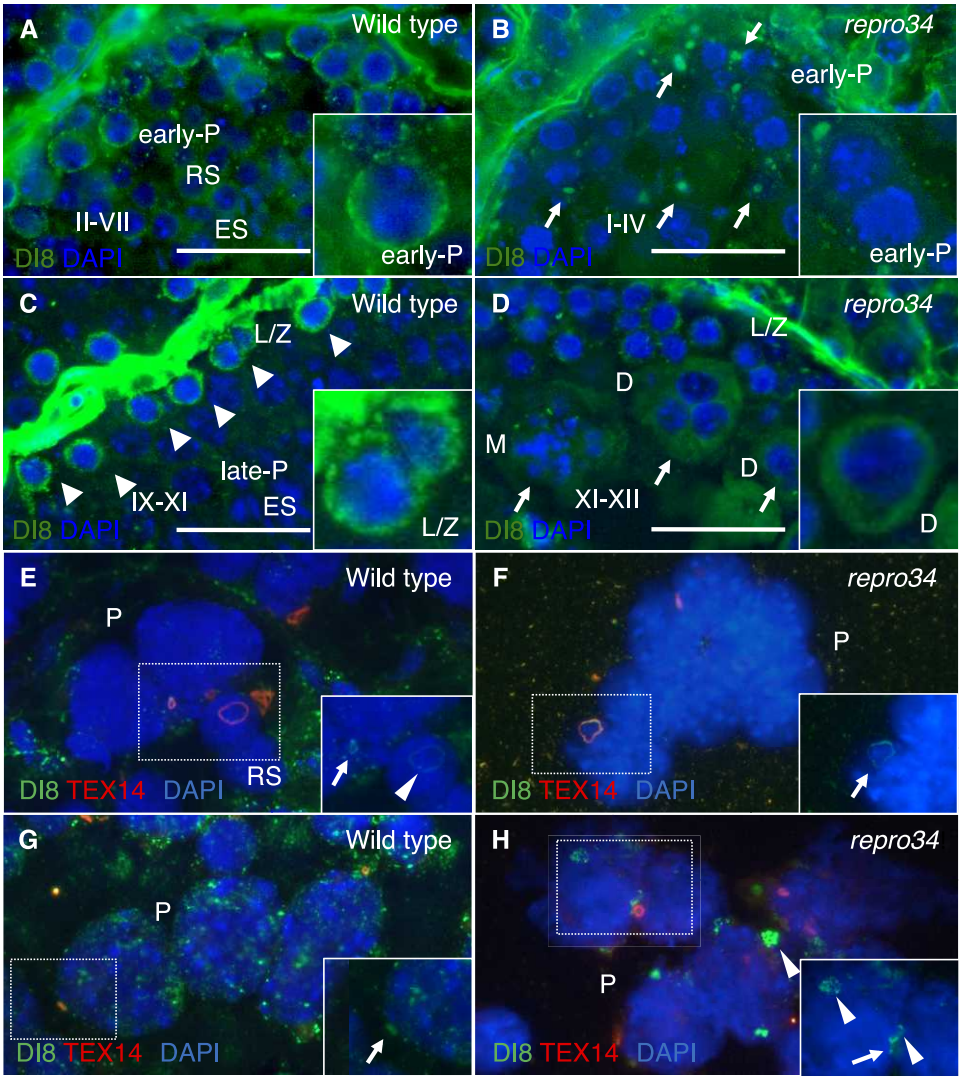

FIG. 5. Localization of sulfoglycolipids in the seminiferous epithelium. **A**, **B**) Granular immunoreaction of sulfoglycolipids (green) was seen in the plasma membrane of early pachytene spermatocytes (**A**) and leptotene/zygotene spermatocytes (arrowheads in **C**). In the *Stx2*^{repro34} mutant, dotty reactions were distributed to the seminiferous epithelium (arrows in **B**). A weak reaction was seen entirely in the cytoplasm of syncytial spermatocytes at the diplotene stage (arrows in **D**). **E**–**H**) Ring-shaped sulfoglycolipid reaction in normal pachytene spermatocytes (arrows in **E**, **G**) and round and elongating spermatids (arrowhead in **E**) obtained by squash preparation showed colocalization with TEX14 (**E**, **G**). Normal pachytene spermatocytes were surrounded by dot sulfoglycolipid reactions (**G**). Sulfoglycolipids were barely observed around *Stx2*^{repro34} mutant pachytene spermatocytes (**F**), but localized to the intercellular bridges (arrows in **F**, **H**). Many *Stx2*^{repro34} mutant pachytene spermatocytes showed abnormal accumulation of sulfoglycolipids around the nucleus (arrowheads in **H**). The nuclei were counterstained with DAPI. Roman numerals show stages of the mouse spermatogenic cycle. L/Z, leptotene or zygotene spermatocytes; P, pachytene spermatocyte; D, diplotene spermatocytes; RS, round spermatid; ES, elongated spermatid. Bar = 50 μm.

ally, in testicular sections we found faint but distinct localization of STX2 to a cytoplasmic organelle corresponding to the morphology and position of the Golgi apparatus in pachytene and diplotene spermatocytes (Supplemental Fig. S5, A, B, and D), as well as to the acrosomal region of the spermatids (Supplemental Fig. S5). That this localization of STX2 was indeed to the Golgi apparatus was confirmed by colocalization of Golgi marker TRA54 in mouse and in rat spermatocytes, where immunostaining was stronger (Supplemental Fig. S5, D and E).

Aberrant Localization of Sulfoglycolipids in Stx2^{repro34} *Mutant Germ Cells*

Sulfoglycolipid deficiency in mice causes spermatogenesis defects morphologically similar to those observed in *Stx2*^{repro34} [10, 11, 14], which led us to speculate that STX2-deficient mice might be impaired in sulfoglycolipid localization. To determine localization of sulfoglycolipids, we used the DI8 mouse monoclonal antibody, which detects both sulfatide and seminolipids containing the terminal 3-O-sulfated galactose structure [19]. In wild-type testes, spermatogonia exhibited very little immunoreactivity (data not shown), while spermatocytes at preleptotene, leptotene/zygotene, and early pachytene stages exhibited a strong and characteristic immunoreaction of fine granular distribution at the peripheral plasma membrane (Fig. 5, A, C, and G). In late pachytene and diplotene spermatocytes and spermatids, labeling in plasma membrane was quite weak and entirely cytoplasmic (Fig. 5C). In addition, spermatocytes and spermatids at any stages, but not spermatogonia, also exhibited ring-shaped sulfoglycolipid localization, which was perfectly colocalized with TEX14 (Fig. 5, E and G).

This reactivity was weak in preleptotene to early pachytene stages and stronger in developing germ cells at later and post-pachytene stages. This confirms that sulfoglycolipids are localized to intercellular bridges in specific developmental stages of spermatogenesis. In *Stx2*^{repro34} mutant testes, spermatogenic cells did not exhibit robust localization of sulfoglycolipids in peripheral plasma membrane (Fig. 5, B, D, F, and H). In addition, an abnormal and patchy intercellular localization was frequently observed at the periphery of mutant pachytene spermatocytes in stages I–IV of the seminiferous epithelium (Fig. 5, B and H). Cytoplasmic accumulation of sulfoglycolipids in mutant spermatocytes at late pachytene and diplotene stages (Fig. 5D) was significantly greater than that of that of wild type (Fig. 5C). Together, these observations suggest aberrant localization and dispersal of sulfoglycolipids in mutant germ cells. Interestingly, sulfoglycolipids were observed in the intercellular bridges of *Stx2*^{repro34} mutant germ cells (Fig. 5, F and H). The diameter of the intercellular bridges between mutant spermatocytes was greater (Fig. 5F) than that of wild type (Fig. 5, E and G), an observation consistent with the opening of the intercellular bridges in *Stx2*^{repro34} mutant spermatocytes.

DISCUSSION

In the present study, we show the expression and subcellular localization of the secretory SNARE protein STX2 in the Golgi apparatus and intercellular bridges of spermatocytes and spermatids. Mice with the *Stx2*^{repro34} mutation do not express STX2 protein and also exhibit abnormalities in the morphology of the intercellular bridges. Furthermore, we show that STX2 colocalizes with sulfoglycolipids in the intercellular bridges. In *Stx2*^{repro34} mutant germ cells, sulfoglycolipids localize to the intercellular bridges but fail to localize to the plasma membrane. The SNARE hypothesis postulates that there are two broad categories of SNARE proteins: the v-SNAREs function in transport vesicles, and the t-SNAREs function in target membranes; the function in both sites is specifically for membrane fusion during exocytosis [36]. STX2 is a t-SNARE protein that functions in secretory granule fusion in pancreatic cells [37], platelets [38], alveolar cells [39], and also in somatic cell cytokinesis [6]. Although these studies suggested the function of STX2 in diverse membrane interaction signaling mechanisms, target molecules have not previously been identified. Taken together, our observations on abnormal intercellular bridge morphology and resultant multinucleation of the *Stx2*^{repro34} mutant germ cells, and the aberrant intercellular distribution of sulfoglycolipids in *Stx2*^{repro34} mutant germ cells, suggest that an STX2-mediated intracellular transport and localization mechanism for sulfoglycolipids could function in the maintenance of intercellular bridges in spermatogenesis.

Meiotic Arrest in Stx2^{repro34} *Mutant Spermatocytes*

Stx2^{repro34} mutant germ cells appear to progress normally through meiosis, and we confirmed normal chromosome synapsis (data not shown) and chiasma formation in the mutant testis (Fig. 3). However, multinucleation of the mutant germ cells occurs in late spermatocytes, with the result that nuclei of several stages—late pachytene, diplotene, and metaphase—were observed in the syncytial germ cells. The presence of syncytial nuclei at metaphase indicates progress of the meiotic division phase under the syncytial condition. However, we did not obtain fetuses or live births after ROSI using the nuclei of the aberrant multinucleated cells, suggesting that either meiosis was not completed or that the mutant germ cells could not support development.

Absence of STX2 in the Golgi Apparatus and Intercellular Bridges Affect Integrity of Intercellular Bridges

STX2 protein is distinctly localized in male germ cells. In wild-type germ cells, perinuclear STX2 localization suggested its presence in the Golgi apparatus or endoplasmic reticulum of spermatocytes, and in the acrosomal vesicle/acrosome of spermatids. This is consistent with a previous report [40]. We did not observe definitive localization of STX2 in the interstitial tissue, such as Leydig cells, in contrast with a previous report [9]. Because we focused on germ cells, we did not pursue discrepancies in interstitial cell localization, which may reflect differences in antibodies or tissue preparation. We also show here localization of STX2 in intercellular bridges, where it is colocalized with the canonical marker of male germ cell bridges, TEX14. The two distinct membrane-rich sites of STX2 localization, the intercellular bridges and the Golgi apparatus, implicate STX2 in membrane dynamics and suggest it could play roles at different developmental stages (Supplemental Fig. S6).

The prominent germ cell phenotype of the *Stx2*^{repro34} mutants is multinucleation. In somatic cell divisions, completion of cytokinesis involves molecular function leading to abscission of the midbody, a central part of the bridge, and failure of cytokinesis triggers multinucleation. Failure of cytokinesis and binucleation in somatic cells were also observed when STX2 and endobrevin, a ubiquitously expressed v-SNARE protein, were functionally impaired, providing evidence that STX2 has a role in mitotic midbody abscission [6]. In contrast, in the testis, germ cell bridges are maintained through many successive cell divisions. Thus, abscission does not occur, but, nonetheless, the bridges are constricted to maintain semi-individuality of the interconnected germ cells undergoing synchronous proliferation and differentiation. Genetic evidence for nonidentity of cells within the syncytium reflects the importance of constricted bridges. Unlike mitotic divisions, the midbodies of germ cell intercellular bridges are maintained by TEX14, via its interaction with CEP55, a component of the midbody, to block midbody abscission [41]. Deficiency of TEX14 causes cytokinesis, resulting in apoptosis of germ cells [34]. In contrast, STX2 deficiency does not promote abscission, but causes an opening of the bridges to produce a multinucleated syncytium of germ cells, suggesting possible loss of membrane rigidity surrounding the bridges. Localization of TEX14 within the *Stx2*^{repro34} mutant syncytial cells (Fig. 2, Fand H) indicates that at least some midbody structures are retained. Two mechanisms for the pathological multinucleation in STX2-deficient germ cells are possible. First, STX2 may play a role in the actual furrowing mechanism, with its deficiency causing enlargement of the cleavage furrow, allowing nuclei to intermingle. Second, STX2 may function in maintaining the integrity of the midbody and/or the adjacent plasma membrane, with its deficiency resulting in failure to maintain a rigid bridge constriction.

STX2 Is Implicated in Intracellular Transportation of Sulfoglycolipids

In either mechanism for loss of intercellular bridge integrity, how might STX2 carry out its function? Our observations on localization of sulfoglycolipids in wild-type and *Stx2*^{repro34} mutant germ cells may give a clue to the role (Supplemental Fig. S7). Here we show that sulfoglycolipids are localized in

the plasma membrane of the wild-type spermatocytes, in agreement with previous reports [12, 42, 43], as wells as in the germ cell intercellular bridges. In mammals, two major sulfoglycolipids, sulfatide and galactosylsulfatide, are produced in the testis by interaction of alkylacylglycerol and ceramide with CST [14, 44] and CGT [10]. The biological importance of sulfoglycolipids in spermatogenesis is revealed by the male-specific infertility of CST- and CGT-deficient mice [10, 11, 14]. Interestingly, there are common morphological characteristics in the testes of CST-, CGT-, or STX2-deficient mice; the multinucleation of spermatocytes at the late pachytene stage suggests that both sulfoglycolipids and STX2 are required for maintenance of intercellular bridges. During spermatogenesis, germ cells experience dynamic morphological changes; late pachytene spermatocytes are larger than those in the previous stages [15], while the diameter of intercellular bridges of spermatocytes remains the same [33]. We postulate that both sulfoglycolipids and STX2 regulate stage-specific membrane dynamics, and our observations of aberrant intracellular localization of sulfoglycolipids in *Stx2*^{repro34} mutant testes are consistent with this hypothesis.

The distinct STX2 localization to the Golgi apparatus we observed also could implicate STX2 as interacting with target sulfoglycolipids, whose biosynthesis in the Golgi membranes also involves CGT catalysis [12]. Sulfoglycolipids form the platform of lipid raft domains that contribute to membrane signaling and trafficking [45] and function in the capacitation of mouse and pig spermatozoa [13, 46]. Mice lacking complex gangliosides, other candidate components of lipid rafts, due to disruption of ganglioside GM2/GD2 synthase also exhibited multinucleation of the spermatids [47, 48], as do STX2-deficient mice. Taken together, these studies lead to the idea that sulfoglycolipids may contribute to raft domains within germ cell plasma membrane and intercellular bridges. Further studies should identify molecules interacting with STX2 and mediating transport of sulfoglycolipids and should analyze membrane domain function in maintaining the constricted intercellular bridges that are a key characteristic of spermatogenesis.

ACKNOWLEDGMENT

Drs. Koichi Honke (Kochi University, Japan), Masaru Okabe (Osaka University, Japan), Bernard de Massy (National Center for Scientific Research, France), Martin M. Matzuk (Baylor College of Medicine, Houston, TX), and Thomas Weimbs (University of California, Santa Barbara, CA) are gratefully acknowledged for gifts of antibodies. We thank Neil Allara for assisting with writing.

REFERENCES

1. Handel MA, Lessard C, Reinholdt L, Schimenti J, Eppig JJ. Mutagenesis as an unbiased approach to identify novel contraceptive targets. Mol Cell Endocrinol 2006; 250:201–205.
2. La Salle S, Palmer K, O'Brien M, Schimenti JC, Eppig J, Handel MA. Spata22, a novel vertebrate-specific gene, is required for meiotic progress in mouse germ cells. Biol Reprod 2012; 86:45.
3. Sun F, Palmer K, Handel MA. Mutation of Eif4g3, encoding a eukaryotic translation initiation factor, causes male infertility and meiotic arrest of mouse spermatocytes. Development 2010; 137:1699–1707.
4. Akiyama K, Akimaru S, Asano Y, Khalaj M, Kiyosu C, Masoudi AA, Takahashi S, Katayama K, Tsuji T, Noguchi J, Kunieda T. A new ENU-induced mutant mouse with defective spermatogenesis caused by a nonsense mutation of the syntaxin 2/epimorphin (Stx2/Epim) gene. J Reprod Dev 2008; 54:122–128.
5. Albertson R, Riggs B, Sullivan W. Membrane traffic: a driving force in cytokinesis. Trends Cell Biol 2005; 15:92–101.
6. Low SH, Li X, Miura M, Kudo N, Quinones B, Weimbs T. Syntaxin 2 and endobrevin are required for the terminal step of cytokinesis in mammalian cells. Dev Cell 2003; 4:753–759.
7. Hutt DM, Baltz JM, Ngsee JK. Synaptotagmin VI and VIII and syntaxin 2 are essential for the mouse sperm acrosome reaction. J Biol Chem 2005; 280:20197–20203.
8. Katafuchi K, Mori T, Toshimori K, Iida H. Localization of a syntaxin isoform, syntaxin 2, to the acrosomal region of rodent spermatozoa. Mol Reprod Dev 2000; 57:375–383.
9. Wang Y, Wang L, Iordanov H, Swietlicki EA, Zheng Q, Jiang S, Tang Y, Levin MS, Rubin DC. Epimorphin(-/-) mice have increased intestinal growth, decreased susceptibility to dextran sodium sulfate colitis, and impaired spermatogenesis. J Clin Invest 2006; 116:1535–1546.
10. Fujimoto H, Tadano-Aritomi K, Tokumasu A, Ito K, Hikita T, Suzuki K, Ishizuka I. Requirement of seminolipid in spermatogenesis revealed by UDP-galactose: ceramide galactosyltransferase-deficient mice. J Biol Chem 2000; 275:22623–22626.
11. Zhang Y, Hayashi Y, Cheng X, Watanabe T, Wang X, Taniguchi N, Honke K. Testis-specific sulfoglycolipid, seminolipid, is essential for germ cell function in spermatogenesis. Glycobiology 2005; 15:649–654.
12. Ishizuka I. Chemistry and functional distribution of sulfoglycolipids. Prog Lipid Res 1997; 36:245–319.
13. Bou Khalil M, Chakrabandhu K, Xu H, Weerachatyanukul W, Buhr M, Berger T, Carmona E, Vuong N, Kumarathasan P, Wong PT, Carrier D, Tanphaichitr N. Sperm capacitation induces an increase in lipid rafts having zona pellucida binding ability and containing sulfogalactosylglycerolipid. Dev Biol 2006; 290:220–235.
14. Honke K, Hirahara Y, Dupree J, Suzuki K, Popko B, Fukushima K, Fukushima J, Nagasawa T, Yoshida N, Wada Y, Taniguchi N. Paranodal junction formation and spermatogenesis require sulfoglycolipids. Proc Natl Acad Sci U S A 2002; 99:4227–4232.
15. Russell LD, Rttlin RA, SinhaHikim AP, Clegg ED. Histological and Histopathological Evaluation of the Testis. Clearwater, FL: Cache River Press; 1990.
16. Chambers TJ. Multinucleate giant cells. J Pathol 1978; 126:125–148.
17. Greenbaum MP, Iwamori T, Buchold GM, Matzuk MM. Germ cell intercellular bridges. Cold Spring Harb Perspect Biol 2011; 3:a005850.
18. Neto H, Collins LL, Gould GW. Vesicle trafficking and membrane remodelling in cytokinesis. Biochem J 2011; 437:13–24.
19. Cheng X, Zhang Y, Kotani N, Watanabe T, Lee S, Wang X, Kawashima I, Tai T, Taniguchi N, Honke K. Production of a recombinant single-chain variable-fragment (scFv) antibody against sulfoglycolipid. J Biochem 2005; 137:415–421.
20. Kotaja N, Kimmins S, Brancorsini S, Hentsch D, Vonesch JL, Davidson I, Parvinen M, Sassone-Corsi P. Preparation, isolation and characterization of stage-specific spermatogenic cells for cellular and molecular analysis. Nat Methods 2004; 1:249–254.
21. Cobb J, Reddy RK, Park C, Handel MA. Analysis of expression and function of topoisomerase I and II during meiosis in male mice. Mol Reprod Dev 1997; 46:489–498.
22. Dobson MJ, Pearlman RE, Karaiskakis A, Spyropoulos B, Moens PB. Synaptonemal complex proteins: occurrence, epitope mapping and chromosome disjunction. J Cell Sci 1994; 107(Pt 10):2749–2760.
23. Dresser ME, Moses MJ. Synaptonemal complex karyotyping in spermatocytes of the Chinese hamster (*Cricetulus griseus*). IV. Light and electron microscopy of synapsis and nucleolar development by silver staining. Chromosoma 1980; 76:1–22.
24. Evans EP, Breckon G, Ford CE. An air-drying method for meiotic preparations from mammalian testes. Cytogenetics 1964; 15:289–294.
25. Fernandez R, Barragan MJ, Bullejos M, Marchal JA, Diaz De La Guardia R, Sanchez A. New C-band protocol by heat denaturation in the presence of formamide. Hereditas 2002; 137:145–148.
26. Klasterska I, Natarajan AT, Ramel C. New observations on mammalian male meiosis. I. Laboratory mouse (*Mus musculus*) and Rhesus monkey (*Macaca mulatta*). Hereditas 1976; 83:203–214.
27. Stock AD, Burnham DB, Hsu TC. Giemsa banding of meiotic chromosomes with description of a procedure for cytological preparations from solid tissues. Cytogenetics 1972; 11:534–539.
28. Wolf KW, Joshi HC. Microtubule organization and distribution of gamma-tubulin in male meiosis of lepidoptera. Mol Reprod Dev 1996; 45: 547–559.
29. Ogonuki N, Inoue K, Hirose M, Miura I, Mochida K, Sato T, Mise N, Mekada K, Yoshiki A, Abe K, Kurihara H, Wakana S, et al. A high-speed congenic strategy using first-wave male germ cells. PLoS One 2009; 4: e4943.
30. Chatot CL, Ziomek CA, Bavister BD, Lewis JL, Torres I. An improved culture medium supports development of random-bred 1-cell mouse embryos in vitro. J Reprod Fertil 1989; 86:679–688.
31. Hamer G, Roepers-Gajadien HL, van Duyn-Goedhart A, Gademan IS, Kal

HB, van Buul PP, de Rooij DG. DNA double-strand breaks and gamma-H2AX signaling in the testis. Biol Reprod 2003; 68:628–634.
32. Huckins C, Oakberg EF. Morphological and quantitative analysis of spermatogonia in mouse testes using whole mounted seminiferous tubules. II. The irradiated testes. Anat Rec 1978; 192:529–542.
33. Weber JE, Russell LD. A study of intercellular bridges during spermatogenesis in the rat. Am J Anat 1987; 180:1–24.
34. Greenbaum MP, Yan W, Wu MH, Lin YN, Agno JE, Sharma M, Braun RE, Rajkovic A, Matzuk MM. TEX14 is essential for intercellular bridges and fertility in male mice. Proc Natl Acad Sci U S A 2006; 103: 4982–4987.
35. Parra MT, Viera A, Gomez R, Page J, Benavente R, Santos JL, Rufas JS, Suja JA. Involvement of the cohesin Rad21 and SCP3 in monopolar attachment of sister kinetochores during mouse meiosis I. J Cell Sci 2004; 117:1221–1234.
36. Rothman JE. Mechanisms of intracellular protein transport. Nature 1994; 372:55–63.
37. Hansen NJ, Antonin W, Edwardson JM. Identification of SNAREs involved in regulated exocytosis in the pancreatic acinar cell. J Biol Chem 1999; 274:22871–22876.
38. Chen D, Lemons PP, Schraw T, Whiteheart SW. Molecular mechanisms of platelet exocytosis: role of SNAP-23 and syntaxin 2 and 4 in lysosome release. Blood 2000; 96:1782–1788.
39. Abonyo BO, Gou D, Wang P, Narasaraju T, Wang Z, Liu L. Syntaxin 2 and SNAP-23 are required for regulated surfactant secretion. Biochemistry 2004; 43:3499–3506.
40. Roqueta-Rivera M, Abbott TL, Sivaguru M, Hess RA, Nakamura MT. Deficiency in the omega-3 fatty acid pathway results in failure of acrosome biogenesis in mice. Biol Reprod 2011; 85:721–732.
41. Iwamori T, Iwamori N, Ma L, Edson MA, Greenbaum MP, Matzuk MM. TEX14 interacts with CEP55 to block cell abscission. Mol Cell Biol 2010; 30:2280–2292.
42. Koul O, Chou KH, Jungalwala FB. UDP-galactose-ceramide galactosyltransferase in rat brain myelin subfractions during development. Biochem J 1980; 186:959–969.
43. Vos JP, Lopes-Cardozo M, Gadella BM. Metabolic and functional aspects of sulfogalactolipids. Biochim Biophys Acta 1994; 1211:125–149.
44. Honke K, Yamane M, Ishii A, Kobayashi T, Makita A. Purification and characterization of 3′-phosphoadenosine-5′-phosphosulfate:GalCer sulfotransferase from human renal cancer cells. J Biochem 1996; 119:421–427.
45. Lingwood D, Simons K. Lipid rafts as a membrane-organizing principle. Science 2010; 327:46–50.
46. Nixon B, Bielanowicz A, McLaughlin EA, Tanphaichitr N, Ensslin MA, Aitken RJ. Composition and significance of detergent resistant membranes in mouse spermatozoa. J Cell Physiol 2009; 218:122–134.
47. Sandhoff R, Geyer R, Jennemann R, Paret C, Kiss E, Yamashita T, Gorgas K, Sijmonsma TP, Iwamori M, Finaz C, Proia RL, Wiegandt H, et al. Novel class of glycosphingolipids involved in male fertility. J Biol Chem 2005; 280:27310–27318.
48. Takamiya K, Yamamoto A, Furukawa K, Zhao J, Fukumoto S, Yamashiro S, Okada M, Haraguchi M, Shin M, Kishikawa M, Shiku H, Aizawa S, et al. Complex gangliosides are essential in spermatogenesis of mice: possible roles in the transport of testosterone. Proc Natl Acad Sci U S A 1998; 95:12147–12152.
49. Grey C, Baudat F, de Massy B. Genome-wide control of the distribution of meiotic recombination. PLoS Biology 2009; 7:e35.
50. Low SH, Miura M, Roche PA, Valdez AC, Mostov KE, Weimbs T. Intracellular redirection of plasma membrane trafficking after loss of epithelial cell polarity. Mol Biol Cell 2000; 11:3045–3060.